Active Vibration Control of Sting Used in Wind Tunnel

Yuke Dai[1], and Xing Shen[2]
Nanjing University of Aeronautics and Astronautics, Nanjing, Jiangsu, 210016, China.

Lei Zhang[3]
Nanjing University of Aeronautics and Astronautics, Nanjing, Jiangsu, 210016, China.

In the design process of an aircraft, the wind tunnel test is usually the main way to obtain relevant aerodynamic parameters. However, in practice, the vibration problem of the long cantilever sting which is used to support the model of aircraft often results in getting inaccurate data and even threatens the safety of the tests. In order to solve this problem, in this paper, a kind of smart cantilever sting based on piezoelectric stacks is proposed, which has the ability to suppress the violent oscillation by active vibration control. Besides, hardware platform is set up and real-time control software is established to launch impulse stimulus to validate the effectiveness of the sting, and it is eventually tested in a low-speed wind tunnel as well as a transonic wind tunnel. The results prove its practical value working at different Mach numbers and angle of attacks, which suggests the superiority of the smart sting and its active vibration control process.

I. Introduction

Wind tunnel is a tubular experimental equipment. During the design process of an aircraft, the wind tunnel test is always a crucial process to get the aerodynamic parameters like lift coefficient, drag coefficient etc. Last decade witnessed the great development of aircraft design and the modern aircrafts have gradually become to share the similar characteristics of light weight, high mobility, enabling high speed and high angle of attack. This obviously requires better design process of the aircraft and less error of the aerodynamic parameters gained from wind tunnel tests. In the actual wind tunnel tests, the sting installed with a test model and a test balance forms an elastic beam. In order to reduce the aerodynamic interference, the slenderness ratio of the sting is designed to be as small as possible. In that case, the damping coefficient of the system decreases dramatically and when the sting is exposed to varying aerodynamic load, large-amplitude and low-frequency vibration would occur easily on the system. Although many structures are vulnerable to vibration in aerospace engineering [1-3], the vibration problem of the sting remains massive hazards, for example, the quality of the collected data deteriorates. Therefore, vibration control of the cantilever sting which is closely related to the success or failure of the experiments is of vital importance.

A great many trials of reducing harmful vibration has been launched. Summarizing from taking passive methods [4-5], people find that the flexibility of which is limited because once the passive damper is manufactured, it is not easy to modify its shape. Therefore, passive methods are not suitable for the standard of wind tunnel tests because the test model is always changing. Accordingly, active vibration control method was proposed because of its good adaptability and many scientists have carried out experiments. For example, Guoliang Ma [6] used the proportional-plus-derivative algorithm and fuzzy algorithm to study the vibration of hoop truss structure in satellite antennas. Ehsan Omidi [7] suppressed the vibration of the piezoelectric cantilever beam by an optimized modified positive velocity feedback control method. Yan-Ru Hu [8] used the piezoelectric patch as the sensor and driver for the vibration of the circular plate and studied the robust controller. Up to now, a great number of researches [9-18] have been conducted and plenty of valuable results have been gained. In the field of wind tunnel tests, the main method to suppress vibration is also the active method.

This paper designs a piezoelectric-stack-based sting for wind tunnel and details its vibration control process. The vibration system including both hardware platform and control software is established. And ground percussion tests as well as the wind tunnel tests are carried out to evaluate the sting and its active vibration control. The results show

[1] Master student, State Key Laboratory of Mechanics and Control of Mechanical Structures, ykdai@nuaa.edu.cn
[2] Professor, State Key Laboratory of Mechanics and Control of Mechanical Structures, shenx@nuaa.edu.cn
[3] Ph.D. student, State Key Laboratory of Mechanics and Control of Mechanical Structures, zhangray@nuaa.edu.cn

that by using the smart sting and active vibration control, the damping coefficient of the system increases 60 times and the working envelope of the wind tunnel expands, which also indicates the reference value of this paper.

II. Illustration of the Smart Sting and Its Vibration Control Process

A. Smart Sting Based on Piezoelectric Stacks

Generally, the sting used in wind tunnel could be regarded as a Bernoulli-Euler beam which ignores the effect of shear deformation. The shape of a normal sting is displayed in Fig. 1. When it is exposed to aerodynamic load, especially in high Mach number and big angle of attacks, the sting section between the test balance and the transition surface may vibrate dramatically. And in practice, the vibration in the pitching direction is the major form of vibration and generally much larger than that of the other two directions (yawing and rolling direction), so the primary target is to suppress the bending moment in the direction of pitching.

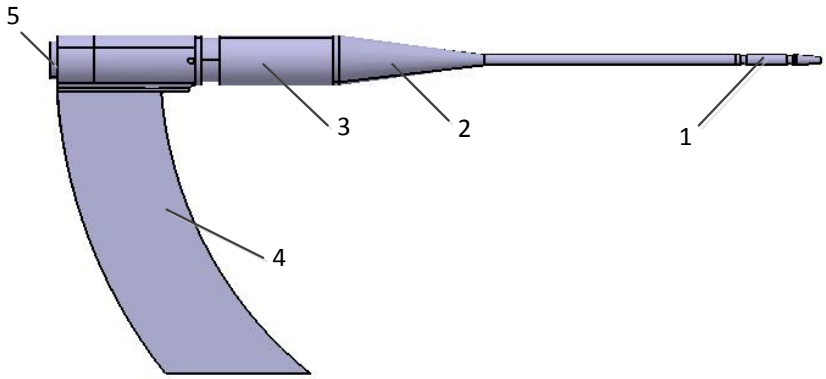

Figure 1. Schematic of the original sting (1-the test balance, 2-the transition surface, 3-the tension joint, 4-the fixed bracket, 5-the tension bolt)

The rising of smart materials guides the way of the design of smart cantilever sting. Piezoelectric material, which has the advantages of quick response, high control precision and reliable operation, is widely used as sensors and actuators. The merits of piezoelectric material reveals its potential in vibration control. Based on it, a structure which focuses on embedding stacked piezoelectric actuators in the sting was proposed by Balakrishna [19]. Inspired by their research, in this paper, a piezoelectric-based sting is designed as shown in Fig. 2. The sting is one meter long and the maximum cross-sectional diameter of structure is 180mm. It is clear that the main change of the structure is the tension joint section. In order to actuate the sting, a pair of piezoelectric stacks is installed at the root of the sting, in front of which is a flexure hinge utilized to amplify the displacement aroused by the stacks. At the tip of the cantilever sting installs a test balance whose function is to measure and transfer the change of aerodynamic load in the pitching direction. Apparently, the principle of the structure is to use the force released by the piezoelectric stacks to suppress the vibration of the cantilever sting, whose direction is opposite to the released force.

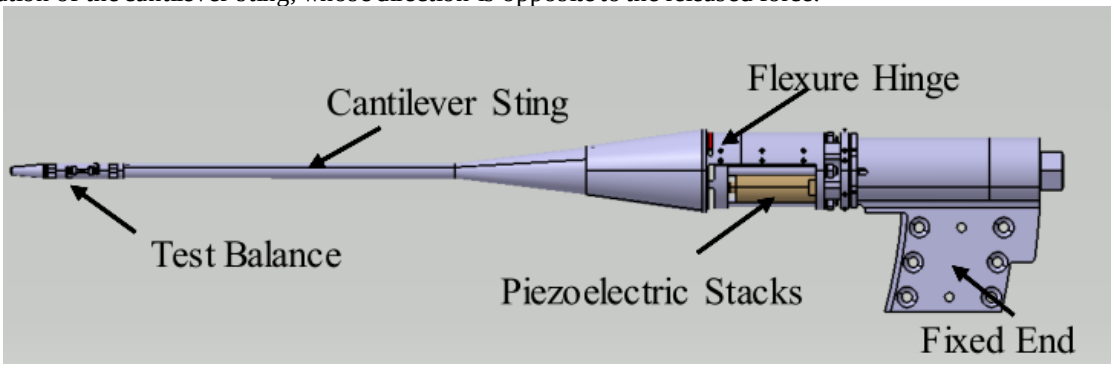

Figure 2. Schematic of the cantilever sting with piezoelectric stacks

In order to ensure the safety of the structure, numerical analysis has been taken on the 3D model of the sting. The following is the results of the static strength analysis using ANSYS software. The material of the structure mainly consists of F141 and 30CrMnSiA. The allowable stress of the material is:

$$[\sigma] = \frac{\sigma_{\max}}{n}, \tag{1}$$

where n is the safety factor. According to the engineering experience, the safety factor of the tension bolt is set at 5, and the safety factor of the rest part is set at 2. In addition, according to the actual working condition, pre-tightening force of 10000N is set for four tightening bolts. The outer load is set at the test balance, which is a maximum static load of 1000N in the pitching direction. And the finite element results are shown in Fig. 3 and Table 1.

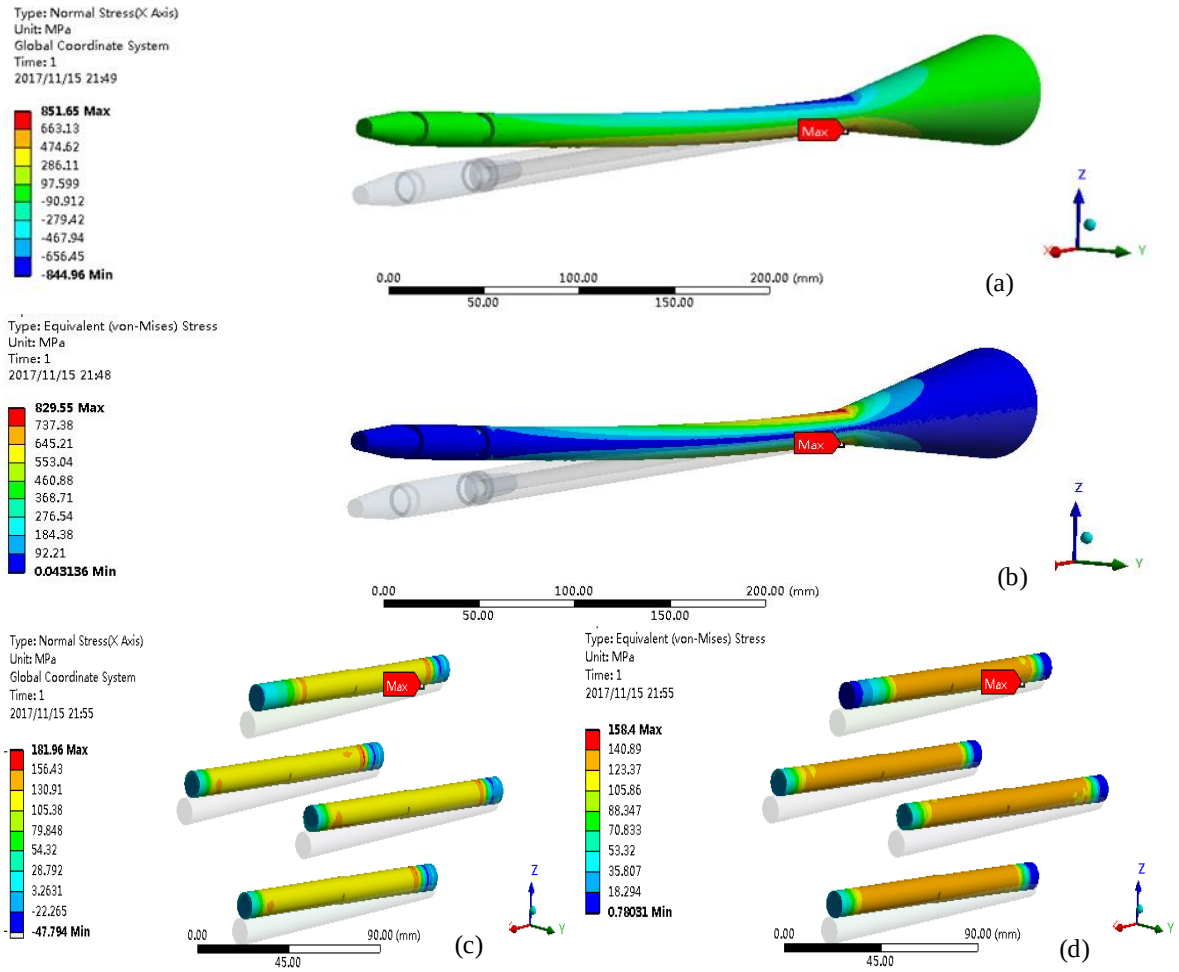

Figure 3. (a) Axial stress nephogram of the sting (b) equivalent stress nephogram of the sting (c) axial stress nephogram of the tension bolts (d) equivalent stress nephogram of the tension bolts

Table 1. Static strength of structures

Structure	Material	Axial stress (MPa)		Equivalent stress (MPa)	
		Max	$[\sigma]$	*Max*	$[\sigma]$
Sting	F141	851.65	931	829.55	861
Tension bolt	30CrMnSiA	181.96	216	158.4	177

Apparently, the static strength of the structure is within the allowable limit of material so that structural failure such as fracture or plastic deformation will not occur even if under the extreme condition.

B. Vibration Control Process

The test balance can be regarded as a mass spring system. After finite element discretization, it can be expressed as:

$$M\ddot{u} + C\dot{u} + Ku = F, \tag{2}$$

where M, C, K are the time-invariant mass, damping and stiffness coefficient matrixes. F is the force vector of the system, which denotes aerodynamic load. With linear proportional damping assumption, the above equation can be converted to equation in modal coordinates:

$$M_q\ddot{q} + C_q\dot{q} + K_q q = \phi^T f, \tag{3}$$

where $q = \{q_1,\ q_2, \ldots, q_n\}^T$ are modal coordinates, and Φ is modal matrix, M_q, C_q, K_q are modal mass matrix, modal damping matrix, modal stiffness matrix respectively. Since all three matrices are diagonal matrices, multi degree of freedom coupled vibrations can be converted into several vibrations of single degree of freedom, which is the essence of independent modal space control. As for the smart sting, the vibration energy mainly concentrates on the first two order mode. Therefore, in this paper, only the vibration of the first two order is considered. And the principle of the sting system is shown in Fig. 4. It is obvious that the key point is applying the restoring moment generated by the piezoelectric stacks to offset the bending moment produced by the airflow.

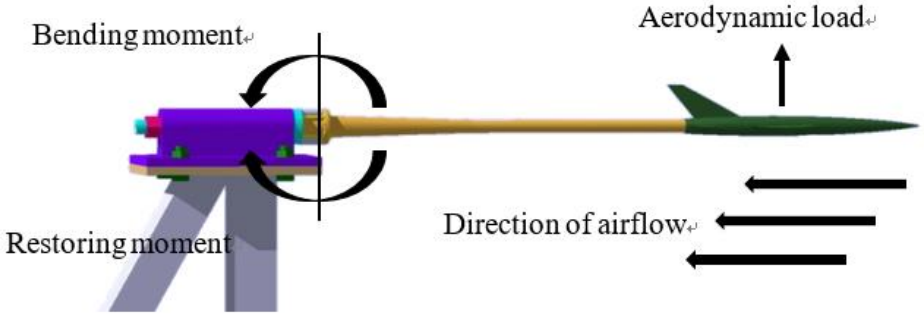

Figure 4 Control principle of the cantilever sting system

And Fig. 5 demonstrates the vibration control process of the whole system. During the test, the aerodynamic model is fixed on the test balance. When aerodynamic load is exerted on the sting, the test balance together with the strain gauge begins to transmit sensed signal. After smoothing by a low pass filter, the signal is sent to the controller, where the control signal is calculated by certain control algorithm. Amplified by a power amplifier, driving voltage is generated and finally, due to reverse piezoelectric effect, the tips of the stacks will stretch slightly and simultaneously push the surface of the flexure hinge so that the restoring moment is produced on the cantilever sting to suppress the vibration of the model. Thus, a negative feedback control system is formed.

In order to release accurate control signal, there are several steps to follow while designing the controller. First of all, modal identification is carried out by broadband excitation. Using the piezoelectric stacks as actuators, the value of first and second modes of the sting system can be gained on the power spectral density (PSD) of the signal from test balance. Then by exciting the structure at the mode frequency, the decoupling matrix can be obtained, which is used for modal decoupling. After that, the two signals from the balance ($u = \{u_1,\ u_2\}^T$) can be decoupled into two uncoupled signal ($q = \{q_1,\ q_2\}^T$). Simultaneously the frequency response function (FRF) could be found, based on which the control signal could be calculated by different control algorithm. In this paper, in order to ensure the feasibility of the system, the most mature and widely-used algorithm, namely classical PD algorithm is chosen.

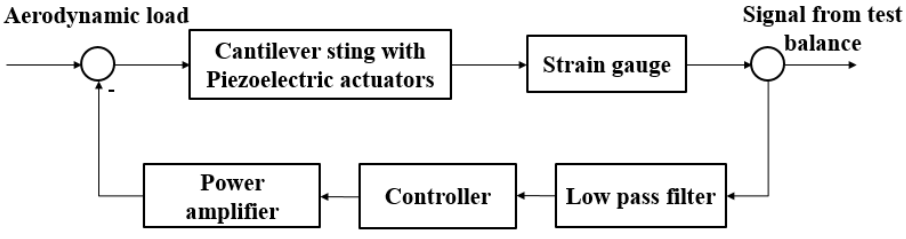

Figure 5 Flow graph of the vibration suppressing process

III. Experimental Setup

In order to evaluate the damping ability of the system. A set of vibration damping system was established as shown in Fig. 6, which involves a controller (PXIe-1071 by National Instruments with a PXI-7841R board card inserted), a strain gauge(SCXI-1520 by National Instruments), a low pass filter (CM3508), a power amplifier(XE509.00 by coremorrow) for the piezoelectric stacks and an smart cantilever sting. As for the piezoelectric stacks, a pair of PSt 1000/25/80 VS35 produced by coremorrow was chosen for its suitable geometry size and the output force. The experimental model chosen in this paper was a scaled model of a fighter designed in China. And in the transonic wind tunnel test, an extra model, which is a scaled model of a guided-bomb invented in China was also applied.

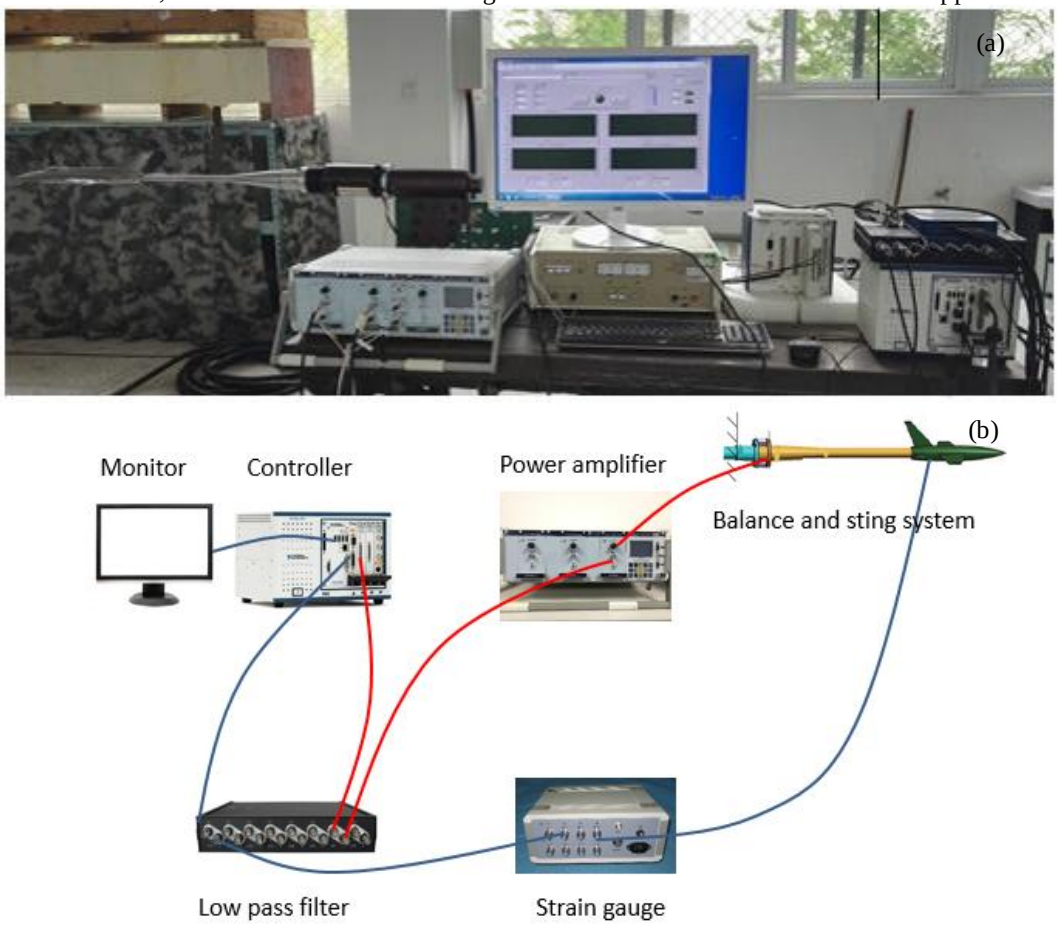

Figure 6 (a) Photograph of the test equipment (b) diagram of the wind tunnel evaluation setup

The whole system was set up at China Aerodynamics Research and Development Center (CARDC). And both impulse verification and wind tunnel test were carried out on this system. The real-time software was established to release and collect experimental data. In addition, the signals were also transmitted to the wind tunnel data acquisition system in order to calculate the value of aerodynamic forces and moments.

IV. Results and Discussion

As discussed above, in order to realize the vibration control, system identification was carried out to find FRF of the sting system. Using ZOOM-FRF algorithm, the FRF was established and information of phase and amplitude at the first two modes was found. Table 2 provides amplitude and phase values calculated at the mode frequencies, based on which the parameters of PD controller could be obtained by the following empirical formula:

$$\sqrt{K_P^2+\left(\omega_r K_D\right)^2}=\frac{1/g-1}{\left|G\left(j\omega_r\right)\right|}$$
$$\arctan\frac{\omega_r K_D}{K_P}=-\angle G\left(j\omega_r\right)+\varphi, \tag{4}$$

Where K_p and K_D are the controlling parameters, ω_r is the identified mode frequency, g is called control effect constant and represents the desired amplitude ratio of input and output signal. By manually adjusting the value of g, different results of PD parameters can be gained. In practice, on the premise that the system does not diverge, the control effect is negatively correlated with the value of g. In this paper, the best values of g we find are 0.05 for Q_1 and 0.1 for Q_2. And the results in the following section are all based on this setting.

Table 2. Amplitude and phase values at mode frequencies (Value on the left side for the fighter and right side for the bomb model)

	Frequency(Hz)		Amplitude		Phase(°)	
Q1	16.11	12.25	4.23	1.41284	33.2	32.096
Q2	50.78	41.8	3.45	1.88734	130.6	45.834

A. Impulse Stimulus

In this section, a hammer was utilized to generate the impulse loading. By knocking vertically on the aerodynamic model, violent oscillation was aroused on the sting. Apparently, if the attenuation time decreases when the controller is on, then the sting system is effective. By collecting the signal from the test balance, the vibration information could be acquired.

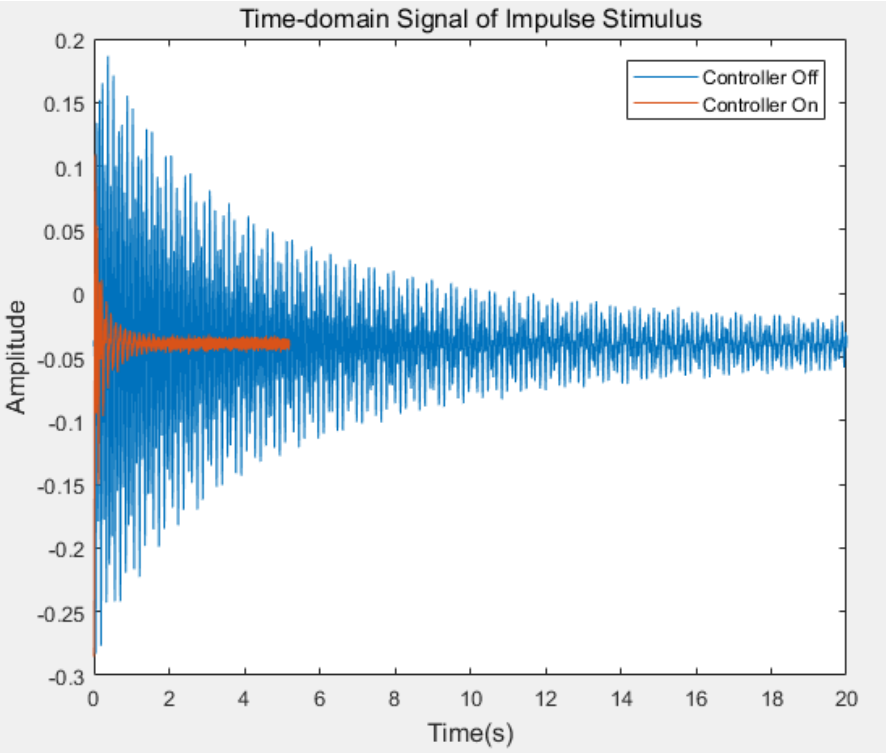

Figure 7 Time-domain signal from test balance with controller on/off

As shown in Fig. 7, it is easy to find when the controller was off, the vibration did not attenuate completely even after 20 s. However, the vibration dramatically decreased in 0.5 s when the controller was on. The result sound supports that the vibration suppression capability of the sting and the controller is excellent. On the other hand, by calculating

the damping coefficients of the structure, we find that compared with the original structure, the damping coefficient rose fleetly as the controller was working. The damping coefficient value of Q_1 is 5.35%, which is 41.15 times larger than that of the uncontrolled structure (only 0.13%). And the damping coefficient value of Q_2 reached 13.53%, which almost enlarges 65 times than the original number (0.21%).

B. Low-speed Wind Tunnel Test

The evaluation of the damping capacity of the sting in low-speed wind tunnel is discussed in this section. Based on the results of the impulse stimulus test on the ground, the purpose of this section is to collect and compare the vibration characteristics of the sting under different airflow speeds. The experimental evaluation was taken in a 0.55 m × 0.4 m low speed acoustic wind tunnel. As shown in Fig. 8, the only difference of the test equipment between the wind tunnel test and the impulse stimulus was the fixed end section. The fixed part of the former is a scimitar-like structure whose mounting angle is adjustable so that the angle of attack in the experiment could be changed. The aim of the test was to reduce the root-mean-square (RMS) value of the vibration signal by more than 50% in different airflow speeds and angles of attack.

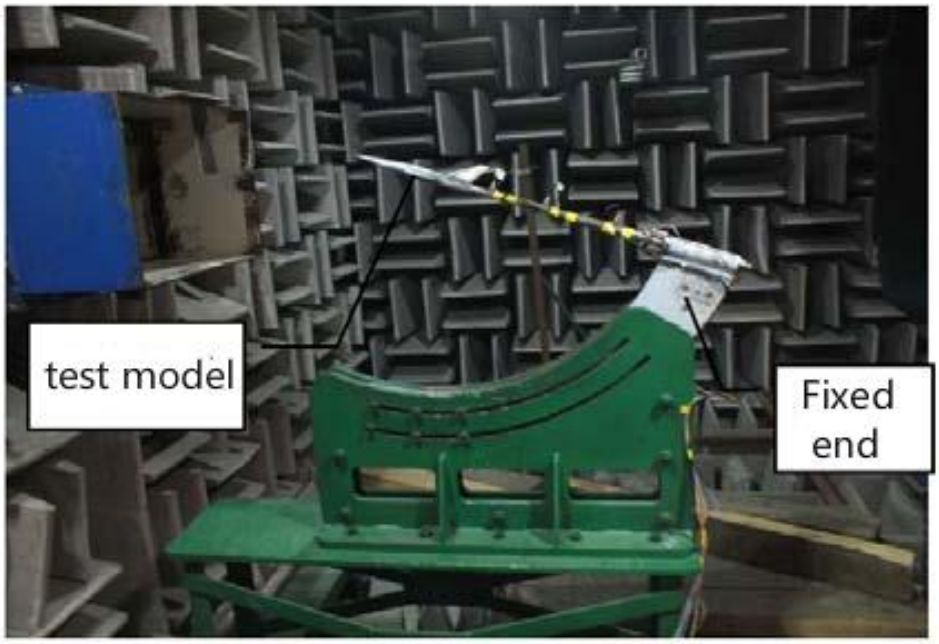

Figure 8 Photograph of the sting fixed in low-speed wind tunnel

The test consists of 8 polars. Every two polars form one controlled experiment. As shown in Table 3, the only difference in each group was the state of the controller. The airflow speeds were set at 15, 20, 25, 30 m/s, and once the airflow speed was determined, the angle of attack was gradually changed from 0 to 20 degree. A sample of the signal collected is presented in Fig. 9. It is easy to find that the overall vibration amplitude was not very large in low-speed wind tunnel whether the controller is on or not, but compared to the free state of vibration, the amplitude reduces dramatically when the controller is running.

Table 3 Configuration information of the low-speed wind tunnel test

Polar No.	Speed(m/s)	Angle of Attack	Controller State
1	15	0,5,10,15,20	OFF
2			ON
3	20	0,5,10,15,20	OFF
4			ON
5	25	0,5,10,15,20	OFF
6			ON
7	30	0,5,10,15,20	OFF
8			ON

And from Fig. 10, in which the RMS value of the signal is demonstrated, the following conclusions can be drawn:

1) As the airflow speed increased, the RMS value soared.
2) The RMS values of the balance signal were almost unchanged with the increase of angle of attack when the airflow speed was determined, which indicates that the effect of angle of attack on the vibration amplitude was not significant.
3) The RMS values after vibration reduction were less than 50% of that before vibration reduction, which achieved the goal, and the results were also not affected by the change of angle of attacks.

After all, the tests manifested the excellent vibration suppression capacity of the sting system and the reliability of the structure was further proved.

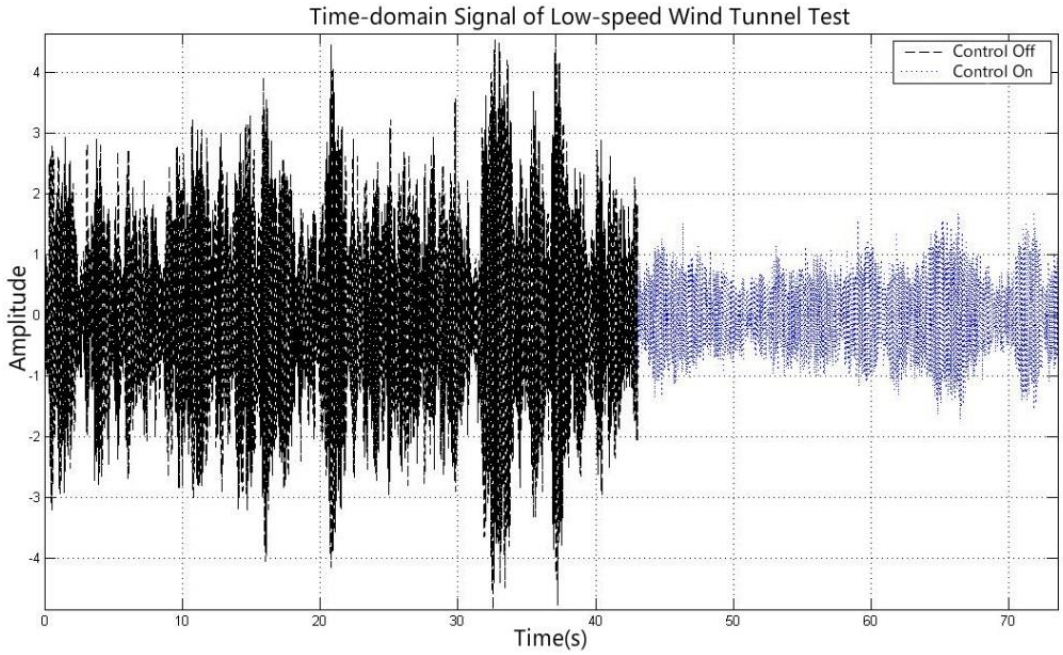

Figure 9 A sample of the signal collected in low-speed wind tunnel test

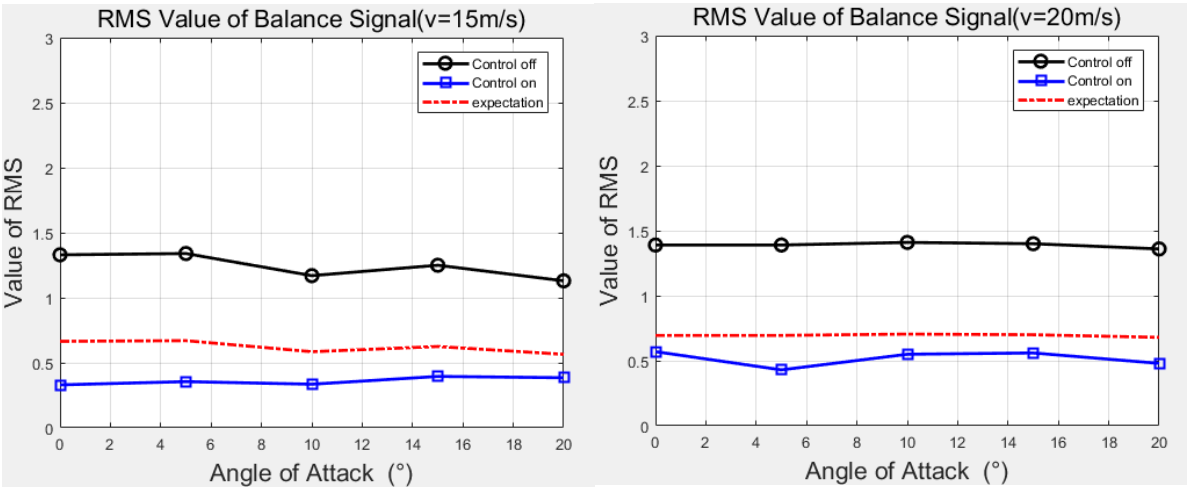

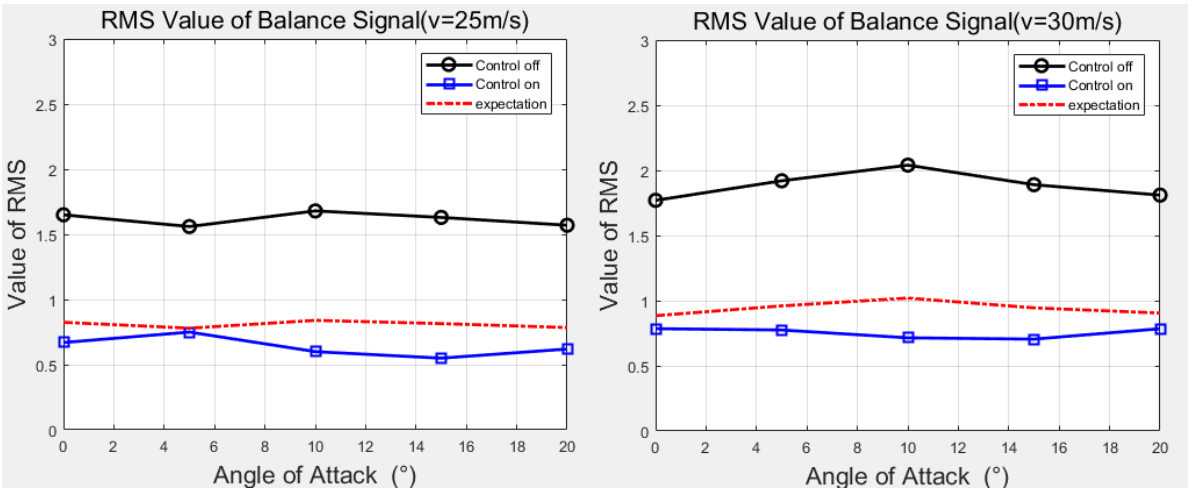

Figure 10 Variation of RMS values with angle of attacks changing under different airflow speed

C. Transonic Wind Tunnel Test

After the evaluation in the low-speed wind tunnel, the system was moved to a 0.6 m × 0.6 m transonic wind tunnel and a series of experiments were carried out. The main process of this section was almost the same as the low-speed wind tunnel tests. Besides, an extra model, which was guided-bomb model was also applied as the test object. Different from the low-speed test, when the velocity of the airflow reaches transonic level, the vibration of the sting might diverge as the angle of attack increased during the test. Therefore, the test would stop immediately when the divergence appears.

The actual flight Mach number of the bomb is around 0.5 and that of the fighter is a little larger. According to this the configuration of each test polar is demonstrated in Table 4. Comparisons of the results are shown in Fig. 11 and 12.

Table 4 Configuration information of the transonic wind tunnel test

Polar No.	Mach	Test Model	Controller State
1	0.4	Bomb	OFF
2			ON
3	0.6	Bomb	OFF
4			ON
5	0.7	Fighter	OFF
6			ON
7	0.8	Fighter	OFF
8			ON

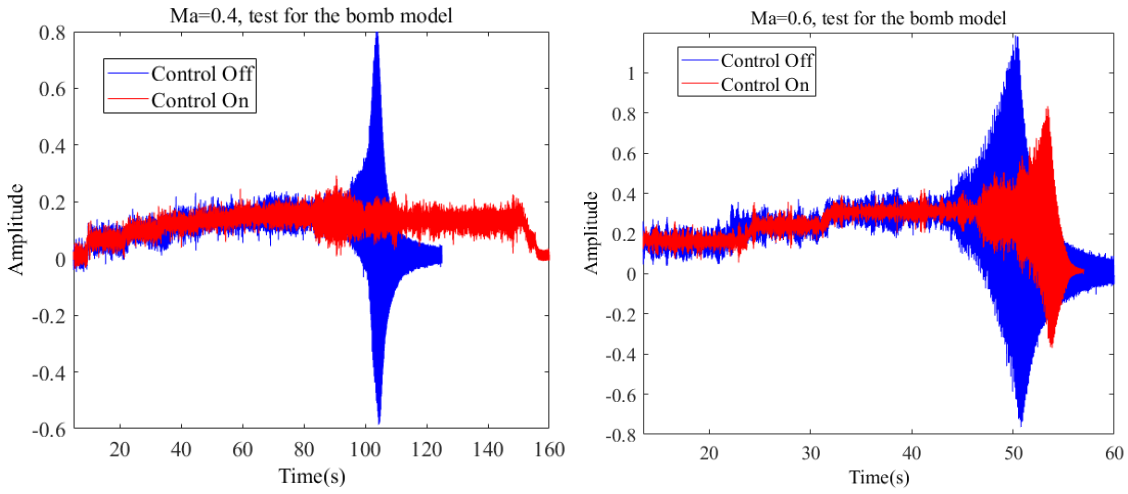

Figure 11 Collected signal from test balance for the bomb model

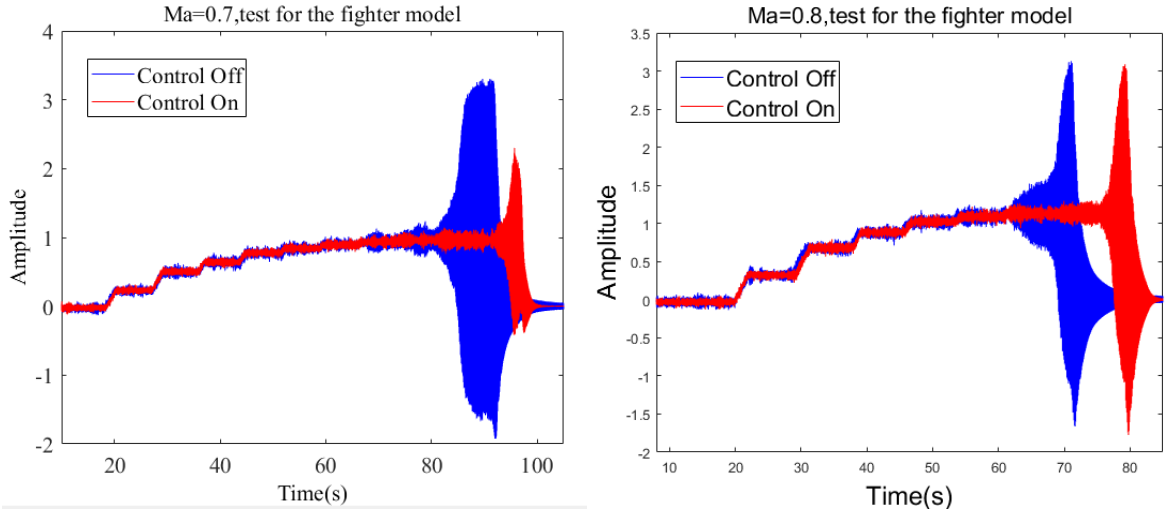

Figure 12 Collected signal from test balance for the fighter model

Among the above 4 figures, the angles of attack increased slightly, and the aerodynamic load as well as the vibration amplitude rose simultaneously. Divergent oscillations could be observed when the angles of attack approached the stall angle and the controller was off. And it is obvious that when the piezoelectric stacks was working, the stall angles increased, which indicates that using the smart sting enlarged the working envelope of the wind tunnel. From Table 5, which displays the value of test angles and the standard deviations at the stall angle, the following conclusion could be drawn:

1) As the Mach number increased, the STD value rose.
2) With comparison of the STD value before and after control, the vibration was suppressed to a great extent. And more than 80% degradation is achieved overall.
3) The working envelope of the test became wider when the controller was working. And apparently, the divergence angle increased with control on and the variation had a negative correlation with the Mach number generally.

Table 5 Results of STD and test angle

Polar No.	STD	STD degradation	Test angle
1	0.4610	97%	0-8°
2	0.0140		0-12°
3	0.6898	82.6%	0-4°
4	0.1202		0-6°
5	1.5777	94.2%	0-15°
6	0.0915		0-17°
7	1.5944	91.6%	0-14.5°
8	0.1302		0-16°

The success of the tests for the two models manifests that the smart sting system have a universal applicability and advantages. And combining the transonic wind tunnel tests together with the former tests, it is claimed that the smart sting is an available tool to tackle the vibration problem in wind tunnel tests.

V. Conclusion

Tackling vibration problem of the support structure is always a vital challenge in wind tunnel tests. In this paper, the concept of a smart sting system which is based on embedding piezoelectric stacks is proposed and analyzed. Besides, a series of evaluation experiments are launched to prove the feasibility and superiority of the system. Applying classical PD control algorithm, the system is finally tested in a low-speed wind tunnel as well as a transonic wind tunnel. The results show that using the piezoelectric stacks as the actuators, the vibration of the sting dramatically reduces and the working envelope of the wind tunnel increases. Besides, the damping coefficient of the sting enlarges over 60 times and the STD value collected in transonic wind tunnel degrades more than 80%. The control effects are satisfactory and finely reach the standard of wind tunnel. The results are in line with expectations and inspires the

confidence for further research, for example, the evaluation of different control algorithms and system identification algorithms.

Acknowledgments

This study was funded by the National Natural Science Foundation of China (No. 11872207).

References

[1] G. L. Ghiringhelli, M. Lanz and P. Mantegazza, "Active flutter suppression for a wing model," Journal of Aircraft, vol. 27, pp. 334-341, 1990.

[2] K. M. Eveker, D. L. Gysling, C. N. Nett, O. P. Sharma, "Integrated control of rotating stall and surge in aeroengines", SPIE Conf. Sensing Actuation and Control in Aeropropulsion, 1995-Apr.

[3] Y. Zhang and X. Guan, "Active damping control of flexible appendages for spacecraft," Aerospace Science and Technology, vol. 75, pp. 237-244, 2018.

[4] W. B. Igoe and F. T. Capone, "Reduction of wind-tunnel-model vibration by means of a tuned damped vibration absorber installed in the model," NASA Technical Memorandum, NASA TMX-1606, 1968.

[5] R. Glaese, G. Bales, S. Hsu, M. Mor, and B. Stirling, "Reduction of Dynamic Response of a Wind Tunnel Sting Mount Using a Hub Damper Unit," in Aiaa Aerospace Sciences Meeting Including the New Horizons Forum & Aerospace Exposition, 2013.

[6] G. Ma, B. Gao, M. Xu, and B. Feng, "Active Suspension Method and Active Vibration Control of a Hoop Truss Structure," AIAA Journal, vol. 56, pp. 1689-1695, 2018.

[7] E. Omidi, S. N. Mahmoodi and W. S. Shepard, "Vibration reduction in aerospace structures via an optimized modified positive velocity feedback control," Aerospace Science and Technology, vol. 45, pp. 408-415, 2015.

[8] Hu and A. Ng, "Active robust vibration control of flexible structures," Journal of Sound and Vibration, vol. 288, pp. 43-56, 2005.

[9] K. L. Roger, G. E. Hodges, and L. Felt, "Active Flutter Suppression—a Flight Test Demonstration," Journal of Aircraft, Vol. 12, no. 6, pp. 551–556, 1975.

[10] T. Nestorovi´ c, N. Durrani, and M. Trajkov, "Experimental Model Identification and Vibration Control of a Smart Cantilever Beam Using Piezoelectric Actuators and Sensors," Journal of Electroceramics, Vol. 29, no. 1, pp. 42–55, 2012.

[11] T. Nestorovi´ c Trajkov, H. Köppe, and U. Gabbert, "Direct Model Reference Adaptive Control (MRAC) Design and Simulation for the Vibration Suppression of Piezoelectric Smart Structures," Communications in Nonlinear Science and Numerical Simulation, Vol. 13, no. 9, pp. 1896–1909, 2008.

[12] T. estorovi´ c, D. arinkovi´ c, G. Chandrashekar, Z. Marinkovi´ c, and M. Trajkov, "Implementation of a User Defined Piezoelectric Shell Element for Analysis of Active Structures," Finite Elements in Analysis Design, vol. 52, pp. 11–22, 2012.

[13] Y. A. Zhuk, I. A. Guza, and C. M. Sands, "Monoharmonic Approximation in the Vibration Analysis of a Sandwich Beam Containing Piezoelectric Layers under Mechanical or Electrical Loading," Journal of Sound and Vibration, Vol. 330, no. 17, pp. 4211–4232, 2011.

[14] C. P. Young, T. G. Popernack, and B. B. Gloss, "National Transonic Facility Model and Model Support Vibration Problems," Proceedings of AIAA 16th Aerodynamic Ground Testing Conference, Seattle, WC, USA, June 1990.

[15] J. Fei, "Active Vibration Control of Flexible Steel Cantilever Beam Using Piezoelectric Actuators," Proceedings of Thirty-Seventh Southeastern Symposium on System Teory, Vol. 5, pp. 35–39, Los Alamitos, CA, USA, March 2005.

[16] L. Li, G. Song, and J. Ou, "Adaptive Fuzzy Sliding Mode Based Active Vibration Control of a Smart Beam with Mass Uncertainty," Structural Control and Health Monitoring, Vol. 18, no. 1, pp. 698–709, 2011.

[17] A. Nandi, S. Neogy, S. Bhaduri, and H. Irretier, "Vibration Attenuation by a Combination of a Piezoelectric Stack and a Permanent Magnet," Shock and Vibration, Vol. 19, no. 4, pp. 719–734, 2012.

[18] X. Shen, Y. K. Dai, M. X. Chen, L. Zhang, and L. Yu, "Active Vibration Control of the Sting Used in Wind Tunnel: Comparison of Three Control Algorithms," Shock and Vibration, vol. 2018, Article ID 1905049, 10 pages, 2018.

[19] S. Balakrishna, H. Houlden, D. Butler and R. White, "Development of a Wind Tunnel Active Vibration Reduction System," Proceedings of 45th AIAA Aerospace Sciences Meeting and Exhibit, pp. 961–974, American Institute of Aeronautics and Astronautics AIAA Associate, Reno, NV, USA, January 2007.